Squaramide Hydroxamate-Based Chemidosimeter Responding to Iron(III) with a Fluorescence Intensity Increase

3 AUTHORS, INCLUDING:

Nathaniel Lim

Avid Radiopharmaceuticals

11 PUBLICATIONS **904** CITATIONS

Christian Brueckner

University of Connecticut

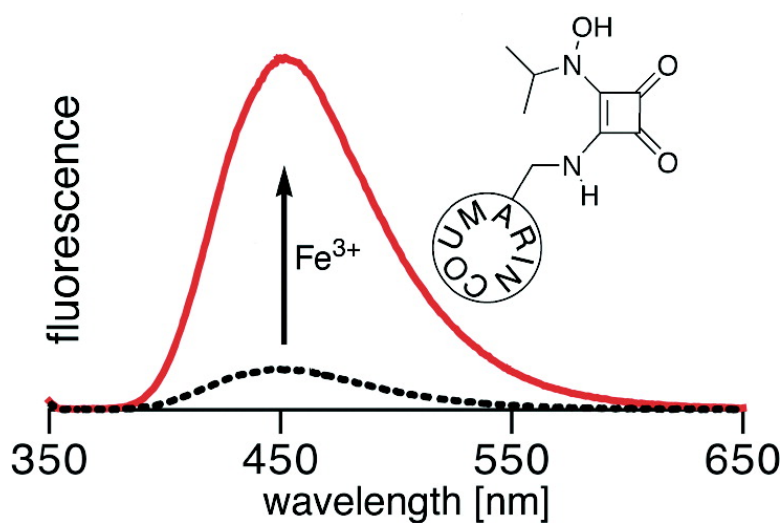**149** PUBLICATIONS **3,610** CITATIONS

Article

Squaramide Hydroxamate-Based Chemidosimeter Responding to Iron(III) with a Fluorescence Intensity Increase

Nathaniel C. Lim, Svetlana V. Pavlova, and Christian Bru#ckner

More About This Article

Additional resources and features associated with this article are available within the HTML version:

- Supporting Information
- Access to high resolution figures
- Links to articles and content related to this article
- Copyright permission to reproduce figures and/or text from this article

View the Full Text HTML

Inorganic Chemistry

Article

Squaramide Hydroxamate-Based Chemidosimeter Responding to Iron(III) with a Fluorescence Intensity Increase

Nathaniel C. Lim,[†,‡] Svetlana V. Pavlova,[‡] and Christian Brückner*

Department of Chemistry, University of Connecticut, Storrs, Connecticut 06269-3060

The synthesis and in vitro evaluation of a squarate hydroxamate−coumarin conjugate, **12**, as a chemodosimeter for Fe(III) and other oxidants, such as Cr(VI) and Ce(IV), is described. As **12** was originally designed to become a chelation-enhanced fluorescence (CHEF)-type sensor for Fe(III), the competence of the squarate diamide platform to relay a CHEF response was demonstrated using a zinc-binding, cyclen-substituted squarate coumarin amide. Due to a photo electron transfer process, **12** possesses a low fluorescence yield. Upon exposure of **12** to Fe(III) (or other oxidants), an irreversible 9-fold fluorescence intensity increase is observed as the result of an oxidation/ hydrolysis reaction. The (aminomethyl)coumarin portion of **12** is oxidized to an iminocoumarin that hydrolyzes to produce a highly fluorescent coumarinaldehyde. Fe(III) acts as a catalyst in this transformation, thereby enhancing the sensitivity of the system for the detection of Fe(III) down to 1 ppm in aqueous buffer solution. The identities of the major reaction products between **12** and Fe(III) were proven by independent synthesis.

Introduction

The availability and careful control of iron is of greatest importance to biological systems as iron deficiencies as well as overloads result in pathological conditions.[1] The amount of bioavailable iron was postulated to be the limiting growth factor in bacterial infections and marine ecosystems.[1,2] Thus, the development of sensitive and iron-selective chemosensors is of greatest interest, particularly as they promise to furnish methods for the monitoring of chelatable iron in living cells or in complex biological media such as seawater.[3,4] Further, immobilized chemosensors are the basis for the development of optical-fiber-based optodes[5] and flow-through detection systems.[6]

A fluorescent metal ion chemosensor comprises a metal ion recognition site and a fluorophore that is triggered upon metal ion binding. For instance, metal binding triggers a fluorescence enhancement (FE) in the sensor, while the unbound molecule is nonfluorescent.[7] One realization of such a "switch-on" probe relies on a photoinduced electron transfer (PET) mechanism.[8] Such a mechanism involves the deactivation of the excited state of a fluorophore by addition of an electron to one of its excited-state frontier orbitals. This leaves the fluorophore in a nonemissive state. For example, the free electron pair of a functional group attached to the fluorophore may quench its fluorescence intramolecularly due to a PET process. Metal coordination to this group renders it a less efficient electron donor, thereby interrupting the PET process. Thus, the native fluorescence of the fluorophore is restored. This mechanism is known as chelation-enhanced fluorescence (CHEF).[7]

* To whom correspondence should be addressed. Fax: (860) 486-2981. Phone: (860) 486-2743. E-mail: c.bruckner@uconn.edu.
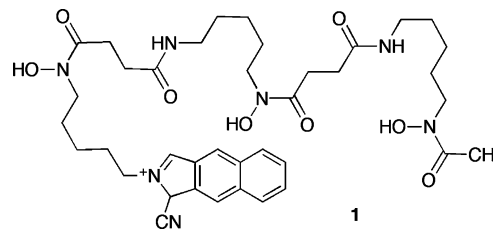† Current affiliation: AVID Radiopharmaceuticals, Philadelphia, PA.
‡ Contributed equally to this work.

(1) (a) Theil, E. C.; Raymond, K. N. In *Bioinorganic Chemistry*; Bertini, I., Gray, H., Lippard, S., Valentine, J., Eds.; University Science Books: Mill Valley, CA, 1994; pp 1−37. (b) Crichton, R. R.; Dexter, D. T.; Ward, R. J. *Coord. Chem. Rev.* **2008**, *252*, 1189−1199. (c) *Iron and Human Disease*; Lauffer, R. B., Ed.; CRC Press: Boca Raton, FL, 1992.
(2) Wells, M. L.; Price, N. M.; Bruland, K. W. *Mar. Chem.* **1995**, *48*, 157−182.
(3) Johnson, K. S.; Coale, K. H.; Jannasch, H. W. *Anal. Chem.* **1992**, *64*, 1065A−1075A.
(4) Domaille, D. W.; Que, E. L.; Chang, C. J. *Nat. Chem. Biol.* **2008**, *4*, 168−174.
(5) Spichinger-Keller, U. E. *Chemical Sensors and Biosensors for Medical and Biological Applications*; Wiley-VCH: Weinheim, Germany, 1998.
(6) Pulido-Tofiño, P.; Bearrero-Moreno, J. M.; Pérez-Conde, M. C. *Talanta* **2000**, *51*, 537−545.
(7) (a) *Fluorescent Chemosensors for Ion and Molecular Recognition*; Czarnik, A. W., Ed.; American Chemical Society: Washington, DC, 1992. (b) Fabrizzi, L.; Poggi, A. *Chem. Soc. Rev.* **1995**, *24*, 197−202. (c) de Silva, A. P.; Gunaratne, H. Q. N.; Gunnlaugsson, T.; Huxley, A. J. M.; McCoy, C. P.; Rademacher, J. T.; Rice, T. E. *Chem. Rev.* **1997**, *97*, 1515−1566. (d) de Silva, A. P.; Fox, D. B.; Huxley, H. J. M.; Moody, T. S. *Coord. Chem. Rev.* **2000**, *205*, 41−57. (e) Rurack, K.; Resch-Genger, U. *Chem. Soc. Rev.* **2002**, *31*, 116−127.

The detection of the paramagnetic d^5 ion Fe(III) (in fact, of any paramagnetic species) using CHEF-type sensors, however, is fraught with an intrinsic problem: Any chelation-induced fluorescence of the fluor is quenched by the proximity of the fluorophore to the paramagnetic metal ion. In turn, the inhibition of the fluorescence emission of a fluorophore brought into close contact with Fe(III) was successfully used in the design for non-PET-type iron-selective chemosensors. The most developed sensors for iron are based on siderophores (or siderophore mimics), polydentate naturally occurring molecules with a marked selectivity for Fe(III), to which a variety of fluorophores were appended (such as 2-cyanonaphtho[2,3-*c*]-2*H*-pyrrolyldes-ferrioxamine B, **1**[9]),[10,11] though other synthetic and biological iron-sensing systems are known.[12−24] Select sensors were shown to be competent in imaging chelatable iron pools in living cells.[11,25] The field of assessing the labile iron pools in biological media using fluorescence methods has been reviewed.[4,26,27] Notwithstanding the success of these sensors, the monitoring of the disappearance of a signal is not ideal, especially as the fluorescence quenching can be caused by a number of factors and, thus, is potentially nonspecific.[28]

To achieve a higher sensitivity for the detection of iron, it is desirable to have a sensor displaying a fluorescence *increase* upon binding of Fe(III). A number of systems achieving this goal were reported in recent years, either by separating the metal-binding moiety and the chromophore, as demonstrated in dendrimeric systems (though no data for Fe(III) were reported),[18] or by employing other than PET mechanisms to result in an FE upon iron binding.[15,16,19,29,30] For instance, one sensor molecule was reported to exhibit significant FE upon (nonspecific) binding of a range of transition metals in nonaqueous, nonprotic solvents.[15] This FE was attributed to multiple effects, among them the preferential solvation of the fluorophore by the water molecules of the hydrated metal salts added. Other systems rely on the chelation-induced change of the $\pi-\pi$ interaction of multiple chromophores,[16] or the chromophore and an electron-rich metal-binding moiety are held sufficiently apart by a rigid linker to allow for a CHEF-type FE.[29]

Recognizing the need for PET/CHEF-type chemosensors for Fe(III), we set out to design such a system. We identified the squarate hydroxamate moiety, first reported by Zinner and Grünefeld in 1985[31] and recently thoroughly explored by us[32] (and, as chelates for zinc, by Seto and co-workers),[33] as a potentially suitable iron-binding platform.

As will be reported here, we failed to realize our goal of creating a reversible CHEF-type sensor for Fe(III) because of the hydrolytic lability and sensitivity toward oxidation of our system. Instead, an irreversible fluorescence enhancement was achieved through the Fe(III)-catalyzed generation of strongly fluorescing chromophores. Thus, the sensor system reported here represents a novel approach toward the realization of a chemidosimeter for Fe(III) (and, as will be detailed below, for other strongly oxidizing metal ions) that, in principle, is related to the "double discrimination" approach recently advanced by Mokhir and Krämer.[20]

(8) Kavarnos, G. J. *Fundamentals of Photo-Induced Electron Transfer*; VCH: Weinheim, Germany, 1993.

(9) Palanché, T.; Marmolle, F.; Abdallah, M. A.; Shanzer, A.; Albrecht-Gary, A.-M. *J. Biol. Inorg. Chem.* **1999**, *4*, 188–198.

(10) (a) Lytton, S. D.; Cabantchik, Z. I.; Libman, J.; Shanzer, A. *Mol. Pharmacol.* **1991**, *40*, 584–590. (b) Barrero, J. M.; Moreno-Bondi, M. C.; Pérez-Conde, M. C.; Cámara, C. *Talanta* **1993**, *40*, 1619–1623. (c) Kikkeri, R.; Traboulsi, H.; Humbert, N.; Gumienna-Kontecka, E.; Arad-Yellin, R.; Melman, G.; Elhabiri, M.; Albrecht-Gary, A.-M.; Shanzer, A. *Inorg. Chem.* **2007**, *46*, 2485–2497.

(11) Epsztejn, S.; Kakhlon, O.; Glickstein, H.; Breuer, W.; Cabantchik, Z. I. *Anal. Biochem.* **1997**, *248*, 31–40.

(12) (a) Bodenant, B.; Fages, F. *Tetrahedron Lett.* **1995**, *36*, 1451–1454. (b) Fages, F.; Bodenant, B.; Weil, T. *J. Org. Chem.* **1996**, *61*, 3956–3961.

(13) (a) Petrat, F.; de Groot, H.; Rauen, U. *Arch. Biochem. Biophys.* **2000**, *376*, 74–81. (b) Petrat, F.; de Groot, H.; Rauen, U. *Biochem. J.* **2002**, *356*, 61–69. (c) Petrat, F.; Weisheit, D.; Lensen, M.; de Groot, H.; Sustmann, R.; Rauen, U. *Biochem. J.* **2002**, *362*, 137–147.

(14) Winkler, J. D.; Bowen, C. M.; Michelet, V. *J. Am. Chem. Soc.* **1998**, *120*, 3237–3242.

(15) Ramachandram, B.; Saroja, G.; Sankaran, N. B.; Samanta, A. *J. Phys. Chem. B* **2000**, *104*, 11824–11832.

(16) Sankaran, N. B.; Banthia, S.; Das, A.; Samanta, A. *New J. Chem.* **2002**, *26*, 1529–1531.

(17) Ouchetto, H.; Dias, M.; Mornet, R.; Lesuisse, E.; Camadro, J. M. *Bioorg. Med. Chem.* **2005**, *13*, 1799–1803.

(18) Grabchev, I.; Chovelon, J.-M.; Qian, X. *New J. Chem.* **2003**, *27*, 337–340.

(19) Tumambac, G. E.; Rosencrance, C. M.; Wolf, C. *Tetrahedron* **2004**, *60*, 11293–11297.

(20) Mokhir, A.; Krämer, R. *Chem. Commun.* **2005**, 2244–2246.

(21) Grabchev, I.; Sali, S.; Betcheva, R.; Gregoriou, V. *Eur. Polym. J.* **2007**, *43*, 4297–4305.

(22) Feng, L.; Chen, Z.; Wang, D. *Spectrochim. Acta, Part A* **2007**, *66A*, 599–603.

(23) (a) Zhang, X.; Shiraishi, Y.; Hirai, T. *Tetrahedron Lett.* **2007**, *48*, 5455–5459. (b) Zhang, M.; Gao, Y.; Li, M.; Yu, M.; Li, F.; Li, L.; Zhu, M.; Zhang, J.; Yi, T.; Huang, C. *Tetrahedron Lett.* **2007**, *48*, 3709–3712.

(24) Crumbliss, A. L. *Coord. Chem. Rev.* **1990**, *105*, 155–179.

(25) (a) Espósito, B. P.; Breuer, W.; Cabantchik, Z. I. *Biochem. Soc. Trans.* **2002**, *30*, 729–732. (b) Ma, Y.; Luo, W.; Quinn, P. J.; Liu, Z.; Hider, R. C. *J. Med. Chem.* **2004**, *47*, 6349–6362.

(26) Espósito, B. P.; Epsztejn, S.; Breuer, W.; Cabantchik, Z. I. *Anal. Biochem.* **2002**, *304*, 1–18.

(27) Reynolds, I. J. *Ann. N.Y. Acad. Sci.* **2004**, *1012*, 27–36.

(28) Lakowicz, J. R. *Principles of Fluorescence Spectroscopy*, 3rd ed.; Springer: New York, 2006.

(29) Bricks, J. L.; Kovalchuk, A.; Trieflinger, C.; Nofz, M.; Büschel, M.; Tolmachev, A. I.; Daub, J.; Rurack, K. *J. Am. Chem. Soc.* **2005**, *127*, 13522–13529.

(30) (a) Hua, J.; Wang, Y.-G. *Chem. Lett.* **2005**, *34*, 98–99. (b) Xiang, Y.; Tong, A. *Org. Lett.* **2006**, *8*, 1549–1552. (c) Zhang, X.-B.; Cheng, G.; Zhang, W.-J.; Shen, G.-L.; Yu, R.-Q. *Talanta* **2007**, *71*, 171–177. (d) Bae, S.; Tae, J. *Tetrahedron Lett.* **2007**, *48*, 5389–5392. (e) Grabchev, I.; Chovelon, J.-M. *Dyes Pigm.* **2007**, *77*, 1–6. (f) Kennedy, D. P.; Burdette, S. C. *Abstracts, 37th Northeast Regional Meeting of the American Chemical Society*, Burlington, VT, June 29 to July 2, 2008; American Chemical Society: Washington, DC, 2008; NERM-118.

(31) Zinner, G.; Grünefeld, J. *Arch. Pharm. (Weinheim, Ger.)* **1985**, *318*, 977–983.

(32) Lim, N. C.; Morton, M. D.; Jenkins, H. A.; Brückner, C. *J. Org. Chem.* **2003**, *68*, 9233–9241.

(33) Onaran, M. B.; Comeau, A. B.; Seto, C. T. *J. Org. Chem.* **2005**, *70*, 10792–10802.

Experimental Section

Instruments and Materials. All solvents and reagents were used as received. (Aminomethyl)coumarin **8** was prepared from commercially available 4-(bromomethyl)-6,7-dimethoxycoumarin (Acros) using a Gabriel synthesis[34] or via a greatly improved pathway, a Deléphine reaction, described below. 1,4,7,10-Tetraazacyclododecane (cyclen) is commercially available (Acros, Strem). Squaric acid derivatives **7**,[35,36] **11a/b**,[32] and **14**[32] were prepared as described before.

The analytical TLC plates were aluminum-backed Silicycle ultrapure silica gel 60, 250 μm, while the flash column silica gel (standard grade, 60 Å, 32−63 mm) used was provided by Sorbent Technologies. ^{1}H and ^{13}C NMR spectra were recorded on a Bruker DRX400. The NMR spectra were referenced to residual solvent peaks or internal TMS. UV−vis spectra were recorded on a Cary 50 spectrophotometer and fluorescence spectra on a Cary Eclipse (both Varian). For the UV−vis and fluorescence studies, concentrated stock solutions of the sensors in DMSO were prepared that were diluted with the buffer solutions indicated. Particularly for sensor **12**, the diluted (aqueous) solutions were freshly prepared for each experiment. Most titrations were performed in disposable polycarbonate cuvettes. If glassware was employed, it was treated with a concentrated, boiling aqueous EDTA solution before use. IR spectra were recorded on a Thermo Nicolet Nexus 670. ESI mass spectra were recorded on a Micromass Quattro II at the University of Connecticut (UConn) Department of Chemistry. High-resolution FAB mass spectra were provided by the Mass Spectrometry Facilities at the Department of Chemistry and Biochemistry, University of Notre Dame, or the UConn Department of Chemistry.

The purity of the novel compounds was assessed by ^{1}H and ^{13}C NMR to be >97% (for copies of the NMR spectra, see the Supporting Information).

Warning! *Liquid, lipophilic squaric acid diesters are known to be potent topical allergens.*[32,37] We did not experience any problems when working with the N-hydroxylamide squarate derivatives. However, we did not test the compounds and habitually exercised great caution when working with these compounds (gloves, transfer of solids only under a well-ventilated fume hood).

4-(Aminomethyl)-6,7-dimethoxy-2*H*-chromen-2-one Hydrochloride (8·HCl). Deléphine Synthesis. To the solution of 4-(bromomethyl)-6,7-dimethoxycoumarin (626 mg, 2.09 mmol) in CHCl$_3$ (30 mL) was added a solution of hexamine (hexamethylenetetramine, urotropin) (445 mg, 3.17 mmol) in CHCl$_3$ (10 mL). The reaction mixture was stirred under N$_2$ at ambient temperature for 24 h. The resulting precipitate was filtered, washed with CHCl$_3$, and air-dried to yield 1-[(6,7-dimethoxy-2-oxo-2*H*-chromen-4-yl)methyl]-3,5,7-triaza-1-azoniatricyclo[3.3.1.1^{3,7}]decane bromide as a yellow solid. Yield: 800 mg (87%). R_f = 0.57 (CHCl$_3$/ 15% MeOH/7.7% Et$_3$N). ^{1}H NMR (DMSO-d_6, 400 MHz, δ): 7.37 (s, 1H), 7.20 (s, 1H), 6.57 (s, 1H), 5.22 (s, 6H), 4.59 (m, 3H), 4.46 (m, 3H), 4.25 (s, 2H), 3.91 (s, 3H), 3.90 (s, 3H) ppm. ^{13}C NMR (DMSO-d_6, 100 MHz, δ): 159.5, 153.3, 149.8, 146.3, 140.2, 119.7, 111.5, 106.6, 100.9, 79.2, 69.7, 57.2, 56.5, 53.6 ppm. This crude product (800 mg, 1.8 mmol) was stirred with a 0.5 M solution of aqueous HCl in EtOH (40 mL) at ambient temperature for 24 h.

The yellow mixture gradually turned white, indicating the completion of the hydrolysis. The precipitate was filtered (glass frit M) and washed with dry EtOH (∼2 mL), followed by Et$_2$O, to yield white microcrystalline **8·HCl**. Yield: 398 mg (93%). R_f = 0.31 (silica−CH$_2$Cl$_2$/10% MeOH). Its spectroscopic and analytical properties were identical to those described previously.[34]

3-{[(6,7-Dimethoxy-2-oxo-2*H*-chromen-4-yl)methyl]amino}-4-methoxycyclobut-3-ene-1,2-dione (9). Method A: A methanolic solution (0.07 M) of free base 4-(aminomethyl)-6,7-dimethoxy-coumarin (**8**) was prepared by addition of a methanolic solution of MeONa (0.5 M, 2 mL) to a solution of 4-(aminomethyl)-6,7-dimethoxycoumarin hydrochloride in MeOH (271 mg in 12 mL of MeOH), followed by filtration of the precipitated NaCl. Method B: A solution of free base (aminomethyl)coumarin **8** in MeOH was prepared from **8·HCl** by addition of a KOH solution in dry MeOH (0.6 M, 0.8 mL) to a solution of **8·HCl** (100 mg, 0.42 mmol) in dry MeOH (5 mL), followed by filtration of the precipitated KCl.

The solutions of free base **8**, prepared via either method A or method B, were combined with an equimolar solution of 3,4-dimethoxycyclobut-3-ene-1,2-dione (**7**) (60 mg) in dry MeOH (1−2 mL). The solutions were stirred at ambient temperature under N$_2$ for 24 h, and the resulting white precipitate was filtered using a glass frit (M), yielding **9** as an off-white solid. Yield: 111 mg, 86% (method B), 58% (method A). R_f = 0.13 (silica−CH$_2$Cl$_2$/20% CH$_3$CN). R_f = 0.6 (silica−CH$_2$Cl$_2$/10% MeOH). Note: A doubling of the signals in the room temperature ^{1}H and ^{13}C NMR spectra of **9** is observed. This is presumably due to a hindered rotation of the N−C$_{square}$ bond, leading to the existence of *E*- and *Z*-type rotamers. Above 50 °C, the doubled signals coalesce (see spectra in the Supporting Information). ^{1}H NMR (DMSO-d_6, 400 MHz, 300 K, δ): 9.27 (s, 1H), 9.05 (s, 1H), 7.18 (br s, 2H), 7.12 (s, 2H), 6.23 (s, 1H), 6.18 (s, 1H), 4.93 (br s, 2H), 4.73 (br s, 2H), 4.32 (s, 3H), 4.24 (s, 3H), 3.87 (s, 6H), 3.85 (s, 6H) ppm. ^{1}H NMR (DMSO-d_6, 400 MHz, 323 K, δ): 8.98 (br s, 1H), 7.21 (s, 1H), 7.09 (s, 1H), 6.21 (s, 1H), 4.84 (br s, 2H), 4.27 (s, 3H), 3.89 (s, 1H), 3.85 (s, 1H) ppm. ^{1}H NMR (DMSO-d_6, 400 MHz, 348 K, δ): 8.88 (br s, 1H), 7.20 (s, 1H), 7.07 (s, 1H), 6.22 (s, 1H), 4.82 (br s, 2H), 4.3 (s, 3H), 3.9 (s, 3H), 3.86 (s, 3H) ppm. ^{13}C NMR (DMSO-d_6, 100 MHz, 300 K, D1 = 5.0 s, LB = 5 Hz, δ): 189.3, 188.8, 182.8, 178.7, 177.4, 172.9, 172.1, 160.3, 152.8, 152.0, 149.0, 146.0, 109.4, 105.3, 100.4, 60.2, 56.2, 56.1, 43.9, 43.4. HR-MS (FAB+ of M$^+$, NBA): *m/z* calcd for C$_{17}$H$_{15}$NO$_7$ 345.0849, found 345.0853.

{4-{2-{[(6,7-Dimethoxy-2-oxo-2*H*-chromen-4-yl)methyl]amino}-3,4-dioxocyclobut-1-enyl}-7,10-bis[(ethoxycarbonyl)methyl]-1,4,7,10-tetraazacyclododec-1-yl}acetic Acid Ethyl Ester (5). Crude squarate **9** (40 mg) was dissolved in CH$_2$Cl$_2$ (20 mL), and 1 equiv of 1,4,7-tris(carboethoxymethyl)-1,4,7,10-cyclododecane **10** in CH$_2$Cl$_2$ (1 mL) was added. The solution was stirred at ambient temperature overnight, and the resulting yellow precipitate was filtered off using a glass frit (M) and air-dried, yielding crude **5** as a yellow solid in 60% yield (52 mg). ^{1}H NMR (DMSO-d_6, 400 MHz, δ): 7.27 (s, 1H), 7,12 (s, 1H), 6.16 (s, 1 H), 4.98 (s, 2H), 4.14 (m, 6H), 3.87 (s, 3H), 3.84 (s, 3H), 3.75−2.67 (m, 18H), 2.01 (s, 2 H), 1.94 (s, 2H), 1.20 (m, 9H) ppm. HR-MS (FAB+ of M$^+$, NBA): *m/z* calcd for C$_{36}$H$_{49}$N$_5$O$_{12}$ 743.3378, found 743.3381.

3-{[(6,7-Dimethoxy-2-oxo-2*H*-chromen-4-yl)methyl]amino}-4-(*N*-isopropylhydroxylamino)cyclobut-3-ene-1,2-dione (12). Method A: **12** was prepared from squarate hydroxamate ester **11b** (266 mg, 1.44 mmol) and free base **8** (2 equiv, 35.75 mL of a 0.8 M solution in MeOH). The methanolic free base 4-(aminomethyl)-6,7-dimethoxycoumarin solution was prepared by addition of a dry methanolic MeONa solution (0.5 M, 5.75 mL) to a solution of **8·HCl** in MeOH (780 mg in 30 mL), followed by filtration of the

(34) Sasamoto, K.; Ushijima, T.; Saito, M.; Ohkura, Y. *Anal. Sci.* **1996**, *12*, 189–193.

(35) Cohen, S.; Cohen, S. G. *J. Am. Chem. Soc.* **1966**, *88*, 1533–1536.

(36) Liu, H.; Tomooka, C. S.; Moore, H. W. *Synth. Commun.* **1997**, *27*, 2177–2180.

(37) Tietze, L. F.; Arlt, M.; Beller, M.; Glüsenkamp, K.-H.; Jähde, E.; Rajewsky, M. F. *Chem. Ber.* **1991**, *124*, 1215–1221.

precipitated NaCl. The solution of the free base amine and the hydroxamate ester was stirred at ambient temperature overnight, and the resulting yellow precipitate was filtered off using a glass frit (M) and dried in a desiccator ($CaCl_2$), yielding **12** as an off-white solid in 32% yield (180 mg). Method B: **12** was prepared from squaric acid monoester monoamide **9** and *N*-isopropylhydroxylamine (*i*-PrNHOH). A solution of free base *i*-PrNHOH in MeOH was prepared by addition of a solution of KOH in dry MeOH (0.6 M, 3.5 mL) to a solution of *i*-PrNHOH·HCl (210 mg, 1.88 mmol) in dry MeOH (1 mL), followed by filtration of the precipitated KCl. The filtrate thus prepared was combined with a solution of squaric acid monoester monoamide **9** (50 mg, 0.145 mmol) in dry MeOH (1 mL) and dry CH_2Cl_2 (10 mL). The solution was stirred at ambient temperature under N_2 to produce a slightly yellow precipitate that was filtered off, washed with MeOH, and dried in a desiccator ($CaCl_2$) to yield **12** as an off-white solid in 48% yield (27 mg). $R_f = 0.55$ (silica−CH_2Cl_2/10% MeOH). Mp: 216−218 °C dec (uncorrected). ^{1}H NMR (DMSO-d_6, 400 MHz, δ): 10.41 (s, 1H), 8.12 (br s, 1H), 7.24 (s, 1H), 7.11 (s, 1H), 6.26 (s, 1H), 4.93 (d, $J = 6.0$ Hz, 2H), 4.39−4.36 (m, 1H), 3.87 (s, 3H), 3.84 (s, 3H), 1.21 (d, $J = 6.5$ Hz, 6H) ppm. ^{13}C NMR (DMSO-d_6, 100 MHz, D1 = 2.5 s, δ): 180.4, 179.3, 167.3, 166.4, 161.0, 153.9, 153.2, 149.4, 146.5, 110.1, 109.7, 105.8, 100.8, 56.7, 56.6, 54.1, 44.2, 19.8 ppm. IR (KBr): ν_{max} 3296 (br), 2939 (br), 1795 (m), 1676 (s), 1593 (s), 1559 (s), 1522 (s), 1283 (s), 1159 (m) 953 (m), 878 (m) cm^{-1}. MS (ES+, 100% H_2O, 30 V): m/z 389 ([M + H]$^+$). MS (ES−, 100% CH_3CN, 30 V): m/z 386.9 ([M − H]$^-$), 422.8 ([M + Cl]$^-$), 774.7 ([M_2 − H]$^-$). MS (FAB+, NBA): m/z 388 (M$^+$, 5), 389 ([M + H]$^+$, 9). HR-MS (FAB+ of [M + H]$^+$, NBA): m/z calcd for $C_{19}H_{21}N_2O_7$ 389.1349, found 389.1352.

3-(Benzylamino)-4-(*N*-methylhydroxylamino)cyclobut-3-ene-1,2-dione (13a). Squarate hydroxamate ester **11a** (600 mg, 3.8 mmol) was dissolved in MeOH (25 mL) and titrated with benzylamine (BnNH$_2$) at ambient temperature (TLC control). Once all the starting material was consumed, the solution was taken to dryness by rotary evaporation, yielding a yellow residue that was recrystallized in hot water and dried in a desiccator ($CaCl_2$) to provide **13a** as a white solid in 72% yield (640 mg). $R_f = 0.21$ (silica−CH_2Cl_2/20% CH_3CN). Mp: 233−237 °C dec (uncorrected). ^{1}H NMR (DMSO-d_6, 400 MHz, δ): 10.62 (s, 1H), 8.14 (br s, 1H), 7.37−7.27 (m, 5H), 4.67 (d, $J = 6.5$ Hz, 2H), 3.33 (s, 3H) ppm. ^{13}C NMR (DMSO-d_6, 100 MHz, D1 = 10 s, δ): 180.9, 179.2, 167.5, 166.9, 140.3, 128.4, 127.6, 127.2, 46.8, 40.8 ppm. IR (KBr): ν_{max} 3320 (br), 2757 (br), 1800 (m), 1672 (s), 1553 (s), 1400 (s), 1354 (s), 1222 (s), 1136 (m), 946 (m), 886 (m) cm^{-1}. MS (ES+, 100% CH_3CN, 30 V): m/z 233 ([M + H]$^+$). MS (FAB+, NBA): m/z 232 (M$^+$, 28), 233 ([M + H]$^+$, 39). HR-MS (FAB+ of [M + H]$^+$, NBA): m/z calcd for $C_{12}H_{13}N_2O_3$ 233.0926, found 233.0924.

3-(Benzylamino)-4-(*N*-isopropylhydroxylamino)cyclobut-3-ene-1,2-dione (13b). 13b was prepared in 81% yield (210 mg) from **11b** and BnNH$_2$ as described for **13a**. $R_f = 0.42$ (silica−CH_2Cl_2/20% CH_3CN). Mp: 176−179 °C dec (uncorrected). ^{1}H NMR (DMSO-d_6, 400 MHz, δ): 10.13 (s, 1H), 8.11 (br s, 1H), 7.38−7.25 (m, 5H), 4.68 (d, $J = 6.6$ Hz, 2H), 4.34−4.32 (m, 1H), 1.17 (d, $J = 6.6$ 6H) ppm. ^{13}C NMR (DMSO-d_6, 100 MHz, D1 = 5 s, δ): 180.4, 178.5, 167.2, 166.1, 139.3, 128.4, 127.6, 127.2, 53.6, 46.8, 19.2 ppm. IR (KBr): ν_{max} 3185 (br), 2926 (br), 1794 (s, C=O), 1650 (s, C=O), 1572 (s), 1428 (m), 1347 (m), 1262 (m), 1168 (m), 750 (s), 698 (s) cm^{-1}. MS (ES+, 100% CH_3CN, 30 V): m/z 261 ([M + H]$^+$). MS (FAB+, NBA) m/z 260 (M$^+$, 38), 261 ([M + H]$^+$, 100), 521 ([M_2 + H]$^+$, 20). HR-MS (FAB+ of [M + H]$^+$, NBA): m/z calcd for $C_{14}H_{17}N_2O_3$ 261.1239, found 261.1244.

3-(Benzylamino)-4-(*N,O*-dimethylhydroxylamino)cyclobut-3-ene-1,2-dione (15). Squarate ester *N,O*-dimethylhydroxamate **14** (160 mg, 0.94 mmol) was dissolved in MeOH (5 mL), and BnNH$_2$ (0.61 mL, 5.6 mmol) was added at ambient temperature. Once all the starting material was consumed (TLC control), the solvent was evaporated and the crude product was recrystallized in hot water and dried in a desiccator ($CaCl_2$), yielding **15** as a white crystalline solid (111 mg, 48% yield). $R_f = 0.72$ (silica−CH_2Cl_2/20% CH_3CN). Mp: 142−146 °C dec (uncorrected). ^{1}H NMR (DMSO-d_6, 400 MHz, δ): 8.28 (br s, 1H), 7.38−7.26 (m, 5H), 4.71 (d, $J = 3.7$ Hz, 2H), 3.68 (s, 3H), 3.38 (s, 3H) ppm. ^{13}C NMR (DMSO-d_6, 100 MHz, D1 = 10 s, δ): 181.6, 178.8, 167.6, 166.0, 139.6, 129.2, 127.9, 127.8, 62.2, 47.3, 37.6 ppm. IR (KBr): ν_{max} 3261 (br), 2935 (br), 1799 (m), 1679 (s), 1576 (s), 1511 (s), 1452 (s), 1347 (s), 966 (m) cm^{-1}. MS (ES+, 100% CH_3CN, 30 V): m/z 247 (MH$^+$). MS (FAB+, NBA): m/z 246 (M$^+$, 40), 247 ([M + H]$^+$, 100). HR-MS (FAB+ of [M + H]$^+$, NBA): m/z calcd for $C_{13}H_{15}N_2O_3$ 247.1083, found 247.1078.

3-(Benzylamino)-4-methoxycyclobut-3-ene-1,2-dione (16). 7 (4.0 g, 28.1 mmol) was dissolved in MeOH (100 mL). BnNH$_2$ (3.25 mL, 29.2 mmol) was added, and the mixture was stirred at ambient temperature for ~1 h. The solution was taken to dryness by rotary evaporation. Column chromatography (silica−CH_2Cl_2/20% CH_3CN) was used to isolate and purify **14** as a white solid (5.1 g, 83% yield). $R_f = 0.60$ (silica−CH_2Cl_2/20% CH_3CN). Mp: 122−124 °C (uncorrected). ^{1}H NMR (DMSO-d_6, 400 MHz, δ): 7.38−7.29 (m, 5H), 4.67 (s, 1H), 4.56 (s, 1H), 4.29 (s, 3H) ppm. ^{13}C NMR (DMSO-d_6, 100 MHz, δ): 189.8, 183.3, 178.0, 173.1, 138.7, 129.0, 127.9, 127.8, 60.3, 47.8 ppm. IR (KBr): ν_{max} 3206 (br, NH), 2952 (m), 2925 (m), 1795 (s, C=O), 1705 (s, C=O), 1594 (s), 1508, (s), 1435 (s), 1408 (s), 1355 (s), 1049 (m), 921 (s), 831 (m), 741 (s), 693 (s) cm^{-1}. MS (ES+, 100% CH_3CN, 30 V): m/z 240 (MNa$^+$). MS (FAB+, NBA): m/z 218 ([MH]$^+$, 51). HR-MS (FAB+ of [MH]$^+$, NBA): m/z calcd for $C_{12}H_{12}NO_3$ 218.0817, found 218.0809.

3-(Benzylamino)-4-(diethylamino)cyclobut-3-ene-1,2-dione (17). Squarate amide ester **16** (220 mg, 1.0 mmol) was dissolved in EtOH (4 mL) and reacted with Et$_2$NH (1.6 mL, 15.5 mmol) under reflux conditions for 5 min. Once all the starting material was consumed, Et$_2$O (3 mL) was added to the hot solution which then was cooled to 0 °C. Crystals were formed overnight and filtered off using a glass frit (M). Washing of the filter cake with cold Et$_2$O and drying under vacuum at ambient temperature afforded **17** in white, crystalline form (0.26 g, 99% yield). $R_f = 0.24$ (silica−CH_2Cl_2/20% CH_3CN). Mp: 175−177 °C (uncorrected). ^{1}H NMR (DMSO-d_6, 400 MHz, δ): 7.38−7.27 (m, 5H), 4.78 (s, 2H), 3.54 (br s, 4H), 1.13 (t, $J = 7.1$ Hz, 6H) ppm. ^{13}C NMR (DMSO-d_6, 100 MHz, D1 = 4 s, LB = 5 Hz, δ): 183.0, 182.2, 167.4, 167.0, 140.0, 128.9, 127.8, 127.6, 46.9, 43.9, 15.5 ppm. IR (KBr): ν_{max} 3203 (br, NH), 2966 (m), 1789 (m, C=O), 1659 (s, C=O), 1570 (s), 1528 (s), 1443 (s), 1315 (m), 1075 (m), 696 (m) cm^{-1}. MS (FAB+, NBA): m/z 258 (M$^+$, 88), 259 ([M + H]$^+$, 99). HR-MS (FAB+ of [M + H]$^+$, NBA): m/z calcd for $C_{15}H_{19}N_2O_2$ 259.1447, found 259.1437.

{[(6,7-Dimethoxy-2-oxo-2*H*-chromen-4-yl)methyl]amino}-4-(isopropylamino)cyclobut-3-ene-1,2-dione (18). Squaric acid monoester monoamide **9** (108 mg, 0.31mmol) was dissolved in a mixture of dry MeOH (6 mL) and CH_2Cl_2 (15 mL), and *i*-PrNH$_2$ (0.125 mL, 4.7 equiv) was introduced by syringe under N_2. The solution was stirred overnight at ambient temperature, and the resulting precipitate was filtered off, washed with dry MeOH, and dried over $CaCl_2$ to yield **18** as white, microcrystalline material. Yield: 90 mg (79%). $R_f = 0.52$ (silica−CH_2Cl_2/10% MeOH). ^{1}H NMR (DMSO-d_6, 400 MHz, 300 K, δ): 7.88 (br, s 1H), 7.68 (br s,

1H), 7.23 (s, 1H), 7.12 (s, 1H), 6.21 (s, 1H), 4.98 (s, 2H), 4.12 (br s, 1H), 3.87 (s, 3H), 3.83 (s, 3H), 1.22 (d, J = 6.49 Hz, 6H) ppm. ^{13}C NMR (DMSO-d_6, 100 MHz, D1 = 5 s, LB = 2 Hz, δ): 183.2 (br), 182.6, 168.1, 167.6 (br), 160.9, 153.8, 153.3, 149.6, 146.5, 110.1, 109.8, 105.8, 100.9, 56.7, 46.3, 43.9, 24.2 ppm. MS (ESI−, 100% CH$_3$CN): m/z 371.0 ([M − H]$^-$, 100), 406.9 ([M + Cl]$^-$, 95). MS (ESI+, 100% CH$_3$CN): m/z 394.9 ([M + Na]$^+$, 435.9 ([M + Na + CH$_3$CN]$^+$). HR-MS (ESI+ of [M + H]$^+$, 100% CH$_3$CN): m/z calcd for C$_{19}$H$_{21}$N$_2$O$_6$ 373.1394, found 373.1410.

Reaction of Sensor 12 with Fe(III) or CAN To Produce Aldehyde 19. Sensor **12** (15 mg, 0.04 mmol) was dissolved in a mixture of MeOH (25 mL) and CH$_2$Cl$_2$ (5 mL), and anhydrous FeCl$_3$ (13 mg, 0.08 mmol) dissolved in MeOH (1 mL) was added dropwise. Addition of the oxidant induces an orange color that pales quickly. After being stirred at ambient temperature for up to 48 h, the reaction mixture was evaporated to dryness by rotary evaporation and separated by column chromatography (silica gel−50% EtOAc/hexanes). The major strongly fluorescing product **19** was isolated as a yellow-orange solid in 56% yield. An equivalent procedure was also adopted for the oxidation of **12** with 2 equiv of [Ce^{IV}(NO$_3$)$_6$](NH$_4$)$_2$ to produce **19** in ∼30% yield. R_f = 0.41 (silica−hexanes/60% EtOAc). ^{1}H NMR (CDCl$_3$, 400 MHz, 300 K, δ): 10.04 (s, 1H), 8.07 (s, 1H), 6.87(s, 1H), 6.73 (s, 1H), 3.95 (s, 3H), 3.94 (s, 3H) ppm. ^{13}C NMR (CDCl$_3$, 125 MHz, D1 = 2.5 s, 300 K, δ): 192.3, 160.9, 153.5, 151.0, 147.0, 143.4, 123.0, 107.2, 106.3, 100.0, 56.4 ppm. MS (ESI+, 100% CH$_3$CN): m/z 235.2 ([M + H]$^+$. The data corresponded to those described previously.[38]

Results and Discussion

Sensor Design Rationale. A chemosensor is composed of a molecular recognition group that is coupled to a reporter group, and an efficient signal transduction between these two moieties has to take place. In squaric acid **2a**, two vinylogous acid moieties are through "cross-conjugation" electronically tightly coupled. This feature makes the squaric acid moiety attractive as a linker between the metal recognition site and the reporter group. The squarate dianion **2b** itself, however, does not bind first- and second-row transition-metal ions in a chelating fashion because the bite angle imposed by the cyclobutene framework is too large to sustain this coordination mode (O−O bite distance of 3.3 Å vs 2.6 Å for the chelating oxalate or hydroxamate anions).[39] As a result, only monodentate binding modes are observed.[40] Monodentate binding is less strong and specific than chelate formation. Therefore, we expanded the chelate by one atom, as in the squarate hydroxamate **3**. This makes chelation from a metric point of view possible (O−O distance 2.8 Å). The vinylogous hydroxamic acid motif was chosen for the known high selectivity of hydroxamates for the binding to Fe(III) that is

also utilized by microorganisms to sequester iron.[39,41] We previously studied the synthesis, structure, and spectroscopic properties of squarate hydroxamate ester **3a** and amide **3b** and related compounds.[32]

Squarate hydroxamate amides provided a weak but positive colorimetric test upon exposure to Fe(III) in aqueous MeOH although crystal structure analyses of the free base chelate have shown that these compounds are not preorganized toward metal binding.[32] Instead, the conformation of the diamides is such that the expected intramolecular H-bond between the *N*-OH functionality and the adjacent carbonyl oxygen is replaced with an intermolecular H-bond (**3c**). This structural feature highlights one crucial difference of **3** from hydroxamic acids, namely, the fact that the *N*-OH functionality and the opposite carbonyl oxygen are in direct conjugation, whereas in hydroxamic acids this is the case with the adjacent carbonyl group. Upon iron chelation to hydroxamates, a fully conjugated metallacycle forms. The vinylogous hydroxamic analogues of type **3** do not possess this driving force for metal chelation, and a weaker binding to iron than for "true" hydroxamic acids can be predicted.
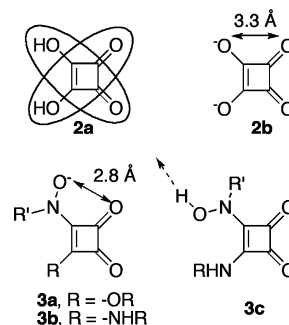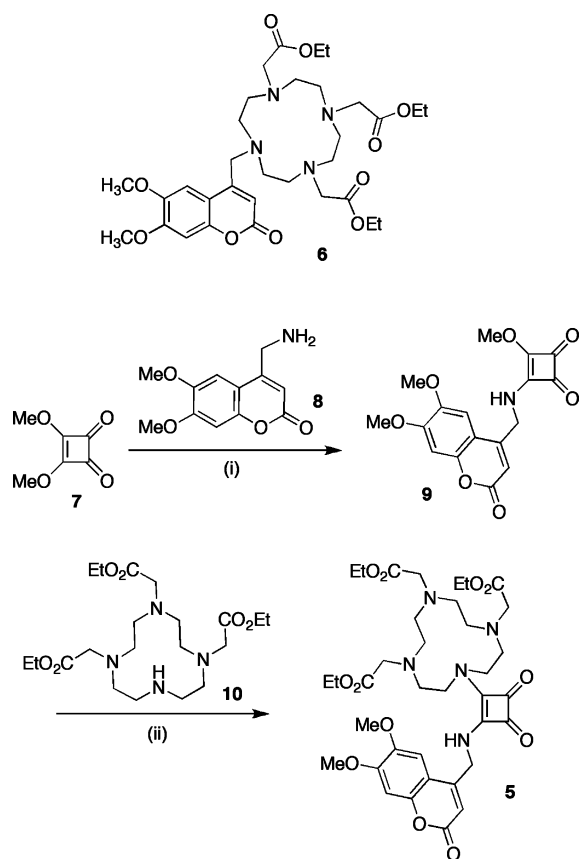

The attachment of a fluorophore opposite the iron-binding site to construct sensor systems of generalized structure **4** is conceptually facile. The amine lone pair on the amine linking the squaramide moiety and the fluorophore will likely cause a PET-type quenching of the chromophore. The linker moiety is also rigid, possibly separating any bound metal from a chromophore attached to its opposite side far enough as to lessen the effects of the paramagnetic quenching of the bound metal. A further advantage with respect to strong signal induction is conceivably derived through the fact that the amine is conjugated with the oxygen atom binding to the iron (**4**−Fe).
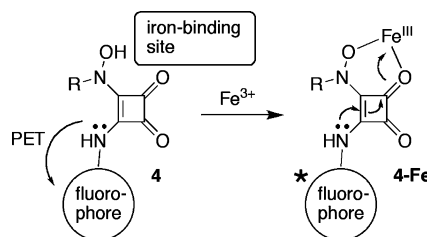
Synthesis of Sensor 5. A squaramide containing an 18-crown-6 ether and an anthracene derivative was reported.[42] Though its design lends itself as a sensor for K$^+$, the sensing properties of this assembly were not revealed. Thus, knowing

(38) Wang, W.; Li, H. *Tetrahedron Lett.* **2004**, *45*, 8479−8481.
(39) Mehrota, R. C. In *Comprehensive Coordination Chemistry*; Wilkinson, G., Gillard, R. D., McCleverty, J. A., Eds.; Pergamon Press: Oxford, U.K., 1987; Vol. 2, pp 505−514.
(40) (a) See, e.g.: Habenschuss, M.; Gerstein, B. C. *J. Chem. Phys.* **1973**, *61*, 852−860. (b) Weiss, A.; Riegler, E.; Robl, C. *Z. Naturforsch., B: Chem. Sci.* **1986**, *41*, 1329−1332. (c) Weiss, A.; Riegler, E.; Robl, C. *Z. Naturforsch., B: Chem. Sci.* **1986**, *41*, 1332−1336. (d) Solans, X.; Aguilo, M.; Gleizes, A.; Faus, J.; Julve, M.; Verdaguer, M. *Inorg. Chem.* **1990**, *29*, 775−784. (e) Khan, M. I.; Chang, Y.-D.; Chen, Q.; Salta, J.; Lee, Y.-S.; O'Connor, C. J.; Zubieta, J. *Inorg. Chem.* **1994**, *33*, 6340−6350. (f) Hilbers, M.; Meiwald, M.; Mattes, R. *Z. Naturforsch., B: Chem. Sci.* **1996**, *51*, 57−67.
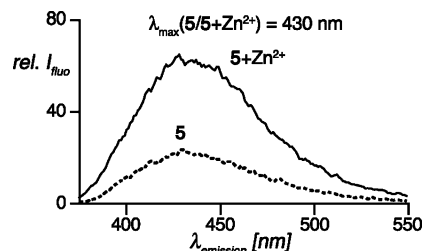
Scheme 1[a]

Figure 1. Native fluorescence intensity of **5** (dashed trace) and that after addition of 1 equiv of Zn^{2+} (solid trace). Conditions: [**5**] = 10 μM in MeOH, $\lambda_{excitation}$ = 345 nm.

[a] Reaction conditions: (i) 1 equiv of **8**, MeOH, 24 h, 25 °C, 58−86% yield; (ii) 1 equiv of **10**, CH$_2$Cl$_2$, 12 h, 25 °C, 60% yield.

that squarate hydroxamate amides bind iron but not having any proof that the squarate moiety is a suitable signal transduction moiety, we synthesized assembly **5** to test this (Scheme 1). This sensor is based on our recently reported coumarin−cyclen CHEF-type chemosensor for Zn(II) **6**,[32,43] expanded by the squaramide signal transduction moiety. A Zn(II) sensor was chosen to unambiguously probe the suitability of the signal transduction moiety in the absence of any possible quenching effects of a bound paramagnetic metal.

Following classic pathways for the synthesis of squarate diamides from squaric acid diesters (such as **7**) by consecutive ester-to-amide exchanges with two different amines, we assembled **5**.[44] Thus, ester-to-amide exchange of squarate dimethyl ester **7** with (aminomethyl)coumarin **8**[34] afforded squarate ester amide **9**. At ambient temperature, the ^{1}H and ^{13}C NMR spectra of **9** show line broadening and doubling of almost all signals in the aliphatic and aromatic regions.

Above 50 °C, the doubled signals coalesce. This effect can be rationalized by an equilibrium between two conformers present in solution, likely caused by a hindered rotation around the N−C$_{squarate}$ bond with the population of both E- and Z-type isomers being about equal (for more information, see the Supporting Information). This observation demonstrates the strong electronic interaction of the nitrogen within its vinylogous amide framework, the prerequisite for the sensor to function as designed.

(Aminomethyl)coumarin **8** and its hydrochloride salt **8**·HCl, prepared by Gabriel synthesis from the corresponding (bromomethyl)coumarin, were described before.[34] However, this reaction was in our hands low yielding (<30% over two steps). Replacing the Gabriel synthesis with a Delépine reaction (nucleophilic substitution of the bromide with hexamethyleneamine, followed by acid hydrolysis), the overall yield for **8**·HCl improved to 81% over two steps.

A second ester-to-amide exchange of **9** with 1,4,7-tris(carboethoxymethyl)-1,4,7,10-cyclododecane **10**[45] generated assembly **5**. This derivative had the expected spectroscopic properties, confirming its assigned structure.

Sensor Properties of 5. Upon addition of Zn^{2+}, **5** exhibited a 2.7-fold increase in fluorescence with no shift in λ_{max} (Figure 1). Hence, the squarate diamide moiety is competent in relaying the zinc-induced PET inhibition from the coordinated nitrogen(s) in the cyclen moiety to the chromophore. However, when compared to sensor **6**, which displays a 4.4-fold FE upon binding to Zn(II),[32,43] a reduction in the FE is noted. This may be either due to inefficient signal transduction through the cyclobutene framework or, more likely, because unbound sensor **5** is already in a partially switched-on state. This is because the cyclen nitrogen attached to the squarate moiety in **5** is a vinylogous amide, whereas the corresponding cyclen nitrogen in **6** is an amine. The nitrogen lone pair in a (vinylogous) amide is partially conjugated into the amide bond and is therefore a much less effective electron source for the PET process. In line with this interpretation, (amidomethyl)coumarins are more than 1 order of magnitude more fluorescent compared to the corresponding PET-quenched (aminomethyl)coumarin,[34] and the fluorescence quantum yield ϕ for **5** was, against the known ϕ of 0.06 for **6**,[43] determined to be 0.15.[46]

Synthesis of Sensor 12. Having established the competency of the squarate diamide moiety with respect to signal transduction, we assembled the coumarin−squarate hydrox-

(41) (a) Codd, R. *Coord. Chem. Rev.* **2008**, *252*, 1387−1408. (b) Dhungana, S.; Crumbliss, A. L. *Geomicrobiol. J.* **2005**, *22*, 87−98. (c) Dertz, E. A.; Raymond, K. N. In *Comprehensive Coordination Chemistry II*; McCleverty, J. A., Meyer, T. J., Eds.; Elsevier: Oxford, U.K., 2004; Vol. 8, pp 141−168. (d) Miller, M. J.; Malouin, F. *Acc. Chem. Res.* **1993**, *26*, 241−249.
(42) Frontera, A.; Orell, M.; Garau, C.; Quiñonero, D.; Molins, E.; Mata, I.; Morey, J. *Org. Lett.* **2005**, *7*, 1437−1440.
(43) Lim, N. C.; Schuster, J. V.; Porto, M. C.; Tanudra, M. A.; Yao, L.; Freake, H. C.; Brückner, C. *Inorg. Chem.* **2005**, *44*, 2018−2030.
(44) Schmidt, A. H. *Synthesis* **1980**, 961−994.

(45) Mishra, A. K.; Chatal, J.-F. *New J. Chem.* **2001**, *25*, 336−339.

Scheme 2[a]
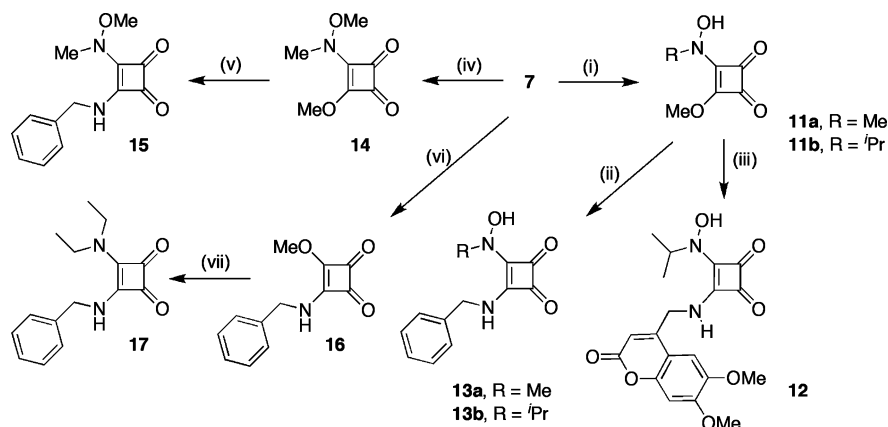
[a] Reaction conditions: (i) hydroxylamine, MeOH, 25 °C;[32] (ii) benzylamine, MeOH, 25 °C, 24 h, 72% yield (for **13a**) and 81% yield (for **13b**); (iii) 4-(aminomethyl)-6,7-dimethoxycoumarin hydrochloride, KOH, MeOH, 25 °C, 24 h, 32% yield; (iv) *N,O*-dimethylhydroxylamine, MeOH, 25 °C, 1 h, 91% yield;[32] (v) benzylamine, MeOH, 25 °C, 24 h, 48% yield; (vi) benzylamine, MeOH, 25 °C, 1 h, 83% yield; (vii) diethylamine, EtOH, reflux, 5 min, 99% yield.

Scheme 3[a]
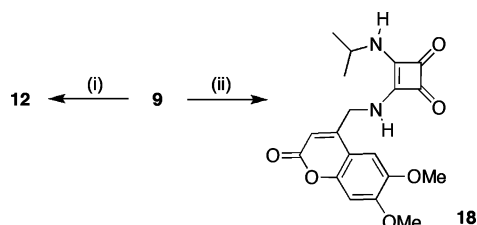
[a] Reaction conditions: (i) 13 equiv of *i*-PrNHOH·HCl, MeOH, CH₂Cl₂, 25 °C, 24 h, 48% yield; (ii) 4.7 equiv of *i*-PrNH₂, MeOH, CH₂Cl₂, 25 °C, 12 h, 79% yield.

amate amide conjugate **12** (Scheme 2). The "southern half" of this sensor is identical to that of sensor **5**, only the metal recognition unit was changed to the squarate hydroxamate moiety. Its synthesis follows the established sequence for squarate hydroxamates:[32] Reaction of squarate diester with a hydroxylamine forms squarate hydroxamate ester **11**, and a subsequent ester-to-amide exchange with (aminomethyl)-coumarin **8** furnishes **12**. Scheme 3 delineates an alternative synthesis of **12** in which the two amidation steps were inverted.[32]

Sensor **12** possesses a fluorescence quantum yield ϕ of 0.04, suggestive of an efficient PET quenching of the coumarin chromophore.[46] As binding models for sensor **12** to Fe(III), we also synthesized hydroxamate amides **13**, **15**, and **17** along similar pathways. All products possess the expected spectroscopic properties.

Reaction of 12, 13, 15, and 17 with Fe(III). The UV−vis spectra of sensor **12** and a number of model compounds in the absence and presence of Fe(III) are shown in Figure 2. The binding of Fe(III) to a hydroxamate, such as *N*-tolylbenzhydroxamic acid, is indicated by the formation of a purple complex. The coloration is due to a CT band in the range between 500 and 650 nm (Figure 2B).[47] Reaction of assembly **12** under identical conditions (1 equiv of Fe(III)

(46) Measured against quinine sulfate in 0.1 M H₂SO₄, $\phi = 0.577$.[28]
(47) Konetschny-Rapp, S.; Jung, G.; Raymond, K. N.; Meiwes, J.; Zähner, H. *J. Am. Chem. Soc.* **1992**, *114*, 2224–2230.
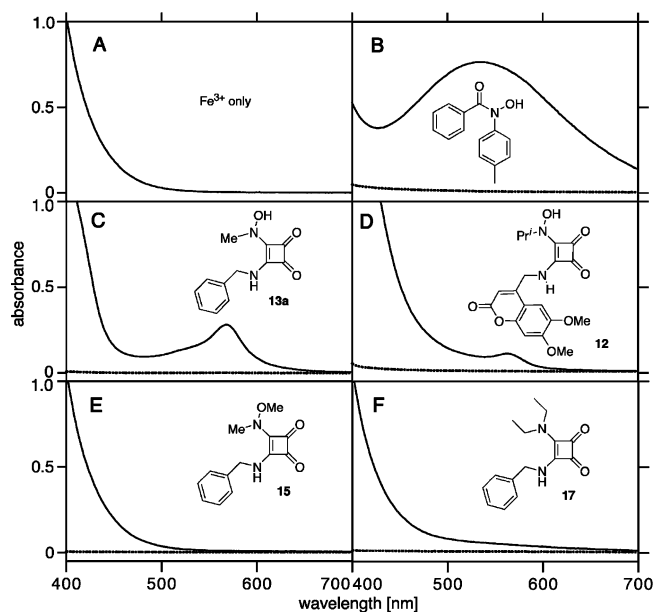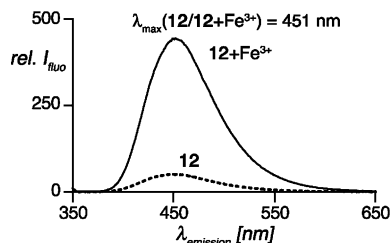

Figure 2. UV−vis spectra of sensor **12**, in comparison to the response of the model compounds indicated, in the absence and the presence of 1 equiv of Fe(III). Conditions: (A) 25 μM FeCl₃ in wet MeOH; (B−F) 25 μM organic compounds in wet MeOH (broken trace), addition of 1 equiv of FeCl₃ (solid trace), immediate measurements.

in wet MeOH) leads to the formation of a pale green color. A weak new band between 550 and 600 nm is observed in the UV−vis spectrum (Figure 2D), but it vanishes within 30 s. A comparable but somewhat longer lived band is observed upon addition of 1 equiv of Fe(III) to a solution of the benzyl derivative **13a** (Figure 2C) or **13b** (not shown). We interpret this colorimetric test as a positive sign for iron binding, followed by chemical reaction(s) (for an analysis of the products of these reactions, see below). Derivative **15** is the methyl-protected hydroxamate **13a**. As expected, this derivative shows no signs of metal binding (Figure 2E). Likewise, the UV−vis spectrum of **17** (Figure 2F) in the presence of 1 equiv of Fe(III) is indistinguishable from the UV−vis spectrum of a methanolic solution of Fe(III), as its chloride (Figure 2A). Furthermore, the amine analogue to

Figure 3. Fluorescence increase of chemosensor **12** upon addition of 1 equiv of Fe(III). Conditions: 139 μM **12** in 0.05 M CH_3CO_2Na buffer, pH 4.4, $\lambda_{excitation} = 347$ nm, 25 °C, aerated solution, equilibration time 15 min. The pH of the solution did not vary significantly upon addition of 1 equiv of Fe(III).

Figure 4. Time-dependent FE of a solution of **12** containing 0.1 equiv of Fe(III). Conditions: [**12**] = 242 μM in 0.05 M CH_3CO_2Na buffer, 0.1 equiv of Fe(III), pH 4.4, $\lambda_{excitation} = 347$ nm, 25 °C, aerated solution.

Figure 5. M^{n+} selectivity profile of sensor **12**: light bars, relative integrated emission intensity of **12** + 1 equiv of M^{n+}; solid bars, relative integrated emission intensity of **12** + M^{n+}, followed by 1 equiv of Fe^{3+}. Conditions: [**12**] = 124 μM in 0.05 M CH_3CO_2Na buffer, pH 4.4, $\lambda_{excitation} = 347$ nm, 25 °C, aerated solutions (except for the test with Fe^{2+}, which was measured in a degassed solution under N_2), equilibration time before measurements 15 min.

12, compound **18** (to be described below), also does not show any indication for the formation of a band in the visible upon addition of Fe(III) (not shown). The behavior of the latter four compounds proves that the coloration observed with **12** or **13** is due to specific binding of the unprotected squaramide hydroxamate moiety to Fe(III). The weaker coloration due to a weaker CT band highlights the differences between "true" hydroxamic acids and the vinylogous hydroxamic acid analogues of type **4** and is likely due to the different electronic factors determining iron binding, as discussed above. The chemical instability of the Fe(III)−squaramide hydroxamate complexes prevented the determination of a stability constant for the binding event (for an investigation of the reaction products, see below). An NMR titration of **12** or **13** with Ga(III) also did not allow the determination of a binding constant, suggestive of a small binding constant for these systems.

Sensor Properties of 12. Addition of an aqueous solution of Fe(III) to a buffered (pH 4.4) aqueous solution of **12** causes a nearly 9-fold enhancement in fluorescence intensity with no concomitant shift of λ_{max} (Figure 3). The extinction coefficient ε at the wavelength of excitation ($\lambda_{excitation} = 347$ nm) for an Fe(III) solution of **12** is 8600 cm^{-1} M^{-1}. The fluorescence quantum yield ϕ of the solution of maximum fluorescence was found to be 0.29.[46] The kinetics of the Fe(III) binding are unexpectedly slow. At a 150 μM concentration of **12** in the presence of 1 equiv of Fe(III) at ambient temperature, equilibration of the FE is reached only after 15 min. The signal does not degrade over the course of 48 h.

These findings were encouraging but also indicated that the system behaved in an untypical manner, and indeed, a number of other observations were incommensurate with a CHEF-type origin of the FE. For example, the FE is irreversible! Addition of a 1000-fold excess of EDTA disodium salt to a solution of **12** + 1 equiv of Fe(III) does not diminish the fluorescence intensity. An extreme binding affinity of **12** to Fe(III) is, given the electronic disadvantages of the squaramide hydroxamates as compared to hydroxamic acids, very unlikely. Kinetic explanations are also unsuitable to rationalize the observed effects. Further, the FE was primarily observed in aqueous, aerated solvents. For instance, addition of Fe(III) to solutions of **12** in dry DMF under N_2 resulted in no FE; in fact, some fluorescence intensity decrease was observed. Lastly, we observed that addition of
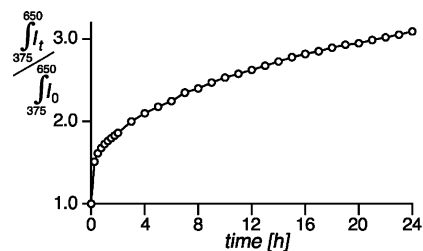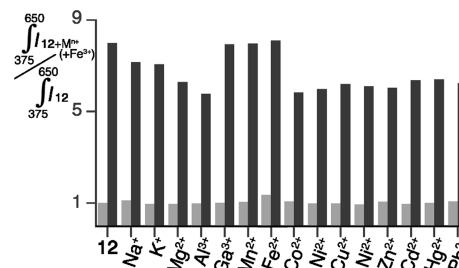
0.1 equiv of Fe(III) to **12** resulted in a steady fluorescence increase over days, ultimately up to an FE value equal to that observed with 1 equiv of Fe(III) after 15 min (Figure 4). This is indicative of a catalytic reaction involving Fe(III). Also, the fluorescence of aqueous aerated solutions of **12** exposed for extended periods of time (days) slowly doubled or tripled even in the absence of added Fe(III), a process inhibited in N_2-flushed solutions, suggestive of an oxidative process responsible for the observed "auto-FE".

Figure 5 shows the results of an M^{n+} selectivity study of **12**. A range of metals was added to buffer solutions of **12**, and no FE or fluorescence quenching was observed. Addition of 1 equiv of Fe(III) to the metal−sensor solutions results in an iron-specific FE of approximately the same magnitude as observed in the absence of the other metal ions. Remarkably, the sensor differentiates between Fe(II) and Fe(III). Particularly the apparent nonbinding to Al(III) and Ga(III) is unusual as these ions often form isostructural complexes with Fe(III).[48]

All these findings taken together point toward a non-CHEF-type mode of operation of derivative **12**.

Fe(III)-Induced Reaction Products of Squarate 12. What mechanism may explain the response profile of squarate **12**? Fe(III) is a strong Lewis acid and potentially a good oxidant. In the following, we will demonstrate that both properties contribute to the observed effects.

As detected by TLC and ESI-MS, the Fe(III)-induced transformation of **12** generates a potpourri of fluorescing and nonfluorescing products. The ESI+-MS spectrum of a solution of **12** shows, inter alia, the signal for $[12 + H]^+$

(48) Karpishin, T. B.; Gebhard, M. S.; Solomon, E. I.; Raymond, K. N. *J. Am. Chem. Soc.* **1991**, *113*, 2977–2984.

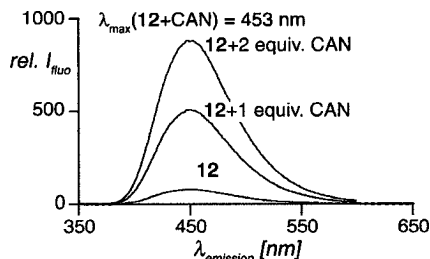**Figure 6.** Fluorescence spectrum of **12** upon reaction with CAN. Conditions: [**12**] = 100 μM in 0.05 M CH$_3$CO$_2$Na buffer, pH 4.4, $\lambda_{excitation}$ = 347 nm, 25 °C, 60 min.

(m/z 389, C$_{19}$H$_{21}$N$_2$O$_7^+$). Increasing amounts of Fe(III) or extended exposure to Fe(III) leads to the appearance of increasingly intense signals at m/z 373, C$_{19}$H$_{21}$N$_2$O$_6^+$, corresponding to a (protonated) deoxygenated product. Parallel to literature precedents,[43] we interpret this as an Fe(III)-catalyzed loss of an oxygen from the hydroxylamine functionality to generate an amine.[49] Could the Fe(III)-induced formation of this hydrolysis product lead to the observed FE?

To test this hypothesis, we synthesized the putative diamide **18** in good yield by reaction of methoxy squarate **9** with *i*-PrNH$_2$ (Scheme 3). Its spectroscopic properties, particularly the replacement of the hydroxylamine hydrogen signal in **12** by an amine hydrogen signal in the ^{1}H NMR spectrum of **18**, proved its successful formation. The removal of the hydroxy group had no effect on the UV−vis or fluorescence spectrum of **18** as compared to the starting material. Much to our surprise, however, amine **18** possesses only about half of the fluorescence yield of **12** (fluorescence quantum yield of 0.02)[54]. Hence, its formation cannot explain the Fe(III)-induced fluorescence of **12**.

The major product formed upon reaction of **12** with Fe(III) is a species with a composition corresponding to the loss of two hydrogens from **12**·H$^+$ (m/z 387, C$_{19}$H$_{19}$N$_2$O$_7^+$), suggestive of an oxidative process. Corroborating this, addition of a dilute aqueous cerium ammonium nitrate (CAN) solution or pyridinium chlorochromate (PCC) to a 100 μM solution of **12** in 0.05 M CH$_3$CO$_2$Na buffer, pH 4.4, leads immediately to an up to 12-fold FE and the formation of the identical m/z 387 product (Figure 6)! Isolation of this product in bulk proved difficult as it decomposed rapidly. In its ^{1}H NMR spectrum it displayed, next to all the signals attributed to the coumarin and the squarate hydroxamate moiety, the loss of the signals assigned to the benzylic methylene protons and the appearance of a new signal at 10.33 ppm. We interpret this as the formation of the imine **20** (Scheme 4). Its major degradation product was shown to be known coumarinaldehyde **19**.[38] Its fluorescence spectrum exactly matches the spectrum shown in Figure 3. We determined its fluorescence quantum yield to be 0.29.[46] Under optimized conditions, oxidation of coumarin squarate **12** with CAN or Fe(III) generates aldehyde **19** in up to 56% isolated yields. Thus, its formation provides an excellent rationalization for

---

Scheme 4[a]
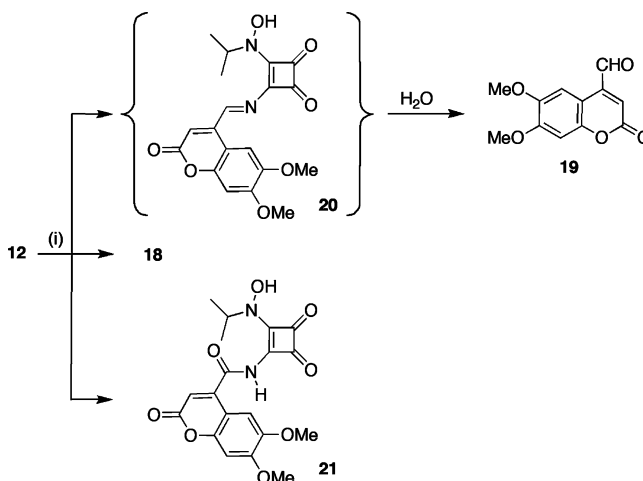
[a] Reaction conditions: (i) 2 equiv of FeCl$_3$ or CAN, MeOH, CH$_2$Cl$_2$, 25 °C, 1−48 h, 30−60% yield of **19**, 5−10% yield of **18** and **21**.
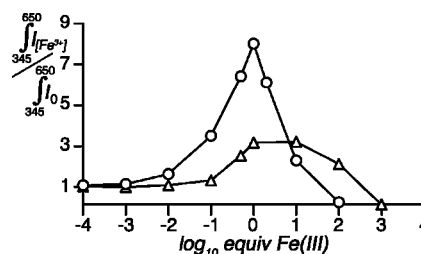

Figure 7. Sensing profile of **12**. Each data point represents a separate sample containing the indicated amounts of Fe(III), measured after 15 min. Conditions: [**12**] = 242 μM (circles) and 2.42 μM (triangles) in 0.05 M CH$_3$CO$_2$Na buffer, pH 4.4, $\lambda_{excitation}$ = 347 nm, 25 °C, aerated solutions.

the observed fluorescence increase upon exposure of **12** to Fe(III) in aerated, aqueous solutions. While it may not be the sole contributor to the observed FE, it is certainly the main contributor. The findings that it is the oxidation ability of Fe(III) that causes the FE explains the ability of **12** to differentiate between Fe(II) and Fe(III).

The formation of a few other minor (∼5%) and brightly fluorescing (on TLC plates) components can also be observed. For instance, one component with an m/z of 403, corresponding to C$_{19}$H$_{19}$N$_2$O$_8^+$, [**12** − 1H + O]$^+$, i.e., the protonated product derived from **12** by loss of two hydrogens and addition of an oxygen, is detectable in the ESI+ spectrum. Considering the chemical structure of **12**, oxidation of the benzylic position to a carbonyl (amide) functionality seemed the most likely reaction. Thus, product **21** was tentatively assigned the structure shown in Scheme 4. Analogous to coumarin amides,[34] this product can be assumed to possess a much higher fluorescence quantum yield than **12**.

The presence of the squarate hydroxamate moiety in **12** proved crucial for the observed oxidation. Neither amine **18** nor protected squarate hydroxamate **9** or coumarin **8** was subject to any oxidative degradation or displayed a fluorescence increase when it was exposed to Fe(III) (under the standard reaction conditions).

Detection Limit for Fe(III) by 12. Since the fluorescence response of **12** is Fe(III)-selective in the absence of other

strongly oxidizing metal ions, the sensor can potentially be used for the chemodosimetric determination of Fe(III). To ascertain the detection limit, we determined the sensitivity of the fluorescence response (Figure 7). The optimal concentration for **12** is in the 100 μM range. At this concentration, the observed maximum increase in fluorescence is about 9-fold after 15 min. At this condition, the lower limit for detection of the Fe^{3+} concentration is 0.01 equiv of Fe(III) (1 μM) while the upper limit is 1.0 equiv (100 μM). Higher concentrations lead to fluorescence quenching. At a lower sensor concentration (2.42 μM), the sensor only produced a 3-fold increase in fluorescence upon addition of 1 equiv of Fe(III) after 15 min. The lower limit at this condition is to a 0.1 equiv of Fe(III) (0.2 μM), while fluorescence quenching is not observed until a 10-fold equivalent (24 μM) of Fe^{3+} is added. Thus, the chemodosimeter **12** in solution is, using fluorimetry, suited to detect levels of Fe(III) down to 1 ppm.

Summary and Conclusions

We set out to design a sensor for Fe(III) that spatially separates a metal-specific binding moiety and the chromophore, yet links them electronically through a squaramide linker. By means of the synthesis of a fluorophore–squarate amide-linked zinc sensor, **5**, we demonstrated the linker to be suitable for signal transduction. Thus, the fluorophore–squarate hydroxamate amide-based Fe(III) sensor **12** was prepared. Though **12** responded to addition of Fe(III) with an FE, this proved to be not, as designed for, due to a CHEF-type mechanism. Instead, reaction of Fe(III) with **12** in aerated aqueous buffers generated a number of products, whereby the major oxidation product, coumarinaldehyde **19**, was shown to be mainly responsible for the observed FE.

We must acknowledge that the results presented here do not provide strong indications of the efficacy of our design.

However, the use of hydrolytically and oxidatively stable binding moieties on this platform may still realize PET/ CHEF-type chemosensory systems. We are currently testing this hypothesis.

On the upside, **12** is suitable for the redox-sensitive chemodosimetric determination of Fe(III) (or other oxidants such as Cr(VI) or Ce(IV)) in aqueous buffer solutions. Using fluorimetry, a 1 ppm detection level for Fe(III) can be achieved. The irreversible sensing mechanism of **12** may also be of advantage in imprinting a permanent image onto (transparent or opaque) polymer films or other objects onto which sensors of type **12** are heterogenized. These optode or indicator films may allow imaging of, for example, the distribution of soluble Fe(III) fractions (and other oxidants) in nontransparent media such as soil cross-sections, thereby collecting data not obtainable with classic chemosensor methods.

Supporting Information Available: ^{1}H and ^{13}C NMR traces of the new compounds **5**, 1-(6,7-dimethoxy-2-oxo-2*H*-chromen-4-ylmethyl)-3,5,7-triaza-1-azoniatricyclo[3.3.1.1[3,7]]decane bromide, **9** (including VT-NMR), **12**, **13a**, **13b**, and **15**−**18** and, for comparison purposes, of known aldehyde **19**. This material is available free of charge via the Internet at http://pubs.acs.org.

IC801322X